Sensors and Materials, Vol. 36, No. 8 (2024) 3407–3418
MYU Tokyo

S & M 3740

Mechanical Characteristics of Al_2O_3, TiCN, and TiAlN Hard Coating Films Measured by Microcantilever Bending Test

Takahiro Namazu,[1*] Tomohide Ide,[2] Tsuyoshi Yamasaki,[3] and Takahito Tanibuchi[4]

[1]Kyoto University of Advanced Science, 18 Yamanouchigotanda-cho, Ukyo, Kyoto 615-8577, Japan
[2]Aichi Institute of Technology, 1247 Yachigusa, Yakusa, Toyota, Aichi 470-0392, Japan
[3]Kyocera Corporation, 45 Wadai, Tsukuba, Ibaraki 300-4247, Japan
[4]Kyocera Corporation, 1810 Taki-cho, Satsumasendai, Kagoshima 895-0292, Japan

(Received May 23, 2024; accepted July 2, 2024)

Keywords: hard coating film, Al_2O_3, TiCN, TiAlN, PVD, CVD, bending test, strength, fracture toughness, internal stress

In this paper, we describe the mechanical characteristics of Al_2O_3 and TiCN thin films formed by chemical vapor deposition (CVD) and a TiAlN thin film formed by physical vapor deposition (PVD), which are used as hard coating films. A focused ion beam (FIB) was used to fabricate a microcantilever beam for strength tests and fracture toughness tests under bending. A nanoindentation system was used to apply normal force to cantilever beams. All the films showed a linear force–deflection relationship, indicating brittle fracture during elastic deformation. The Young's modulus ranged from 340 to 379 GPa, with no significant difference among the films, whereas the fracture strength of the Al_2O_3 films was 5.5 GPa, which was almost twice those of the other two films. For the fracture toughness test, a precrack with various depths was made using FIB at 2 μm from the fixed end of the cantilever beam. The Al_2O_3 film toughness values ranged from 4.1 to 5.5 MPa$\sqrt{m}$, which were almost twice that of the TiCN film at each precrack depth. Both CVD films showed a similar trend, i.e., an increase in fracture toughness with decreasing precrack depth, However, the fracture toughness of the TiAlN film showed no precrack depth dependence. The difference in fracture toughness between the CVD and PVD films is discussed on the basis of fracture surface observation results and information on the crystal grain size and orientation.

1. Introduction

Hard coating films such as Al_2O_3, TiCN, and TiAlN films play an important role in preventing the chipping and wearing of cutting tools, leading to the improvement of their long-term durability and reliability.[1–5] Improving the adhesion of a coating film to a tool is one of the significant concerns to overcome delamination. Also, investigating the mechanical properties such as Young's modulus, fracture strength, and fracture toughness is significant for realizing the high performance and reliability of a film-coated cutting tool. For thin films, many

*Corresponding author: e-mail: namazu.takahiro@kuas.ac.jp
https://doi.org/10.18494/SAM5152

ISSN 0914-4935
https://myukk.org/

researchers have developed their original tensile mechanical testing technologies.[6–15] Shaping and chucking a film sample are considered the technical challenges for thin-film tensile testing. Tsuchiya *et al.* proposed an electrostatic chucking technique, which is effective mainly for semiconductor solid films because the sample is produced using microfabrication technologies.[6] Sato *et al.* developed an on-chip tensile test chip, which includes a thin-film sample, torsion beams, and loading levers.[7] The technique is advantageous because no chucking process is necessary, and it can be applied to single-crystal Si and Si-related materials because those mechanical components are batch-processed. We developed a mechanical chucking technique with a pin-hole combination, which can be applied to various types of thin-film material if a sample, consisting of a thin-film section, chucking holes, Si springs for supporting a movable part, and frame, can be prepared using microfabrication technologies.[8–15] Although those techniques are sophisticated, it is difficult to use them for evaluating hard coating films because sample preparation is technically difficult owing to their hardness and chemical inertness.

The focused ion beam (FIB) is a powerful tool for directly fabricating materials to a 3D shape without photolithography and etching. It works well for making a mechanical test piece with a wire shape even if the material is difficult to process.[16–20] The purpose of this study is to establish a strength and fracture toughness evaluation method for hard-coating thin-film materials and to compare the mechanical characteristics among Al_2O_3, TiCN, and TiAlN films. FIB was utilized to prepare a microscale cantilever beam made of those film materials. A microcantilever bending test was performed using a nanoindentation system.

2. Experimental Procedure

Figure 1 shows photographs of Al_2O_3, TiCN, and TiAlN films deposited on a machine tool along with their surface photographs. WC-Co was used as the deposition substrate, which is typically used for a machine tool. The one-side length in-plane and thickness of the substrate

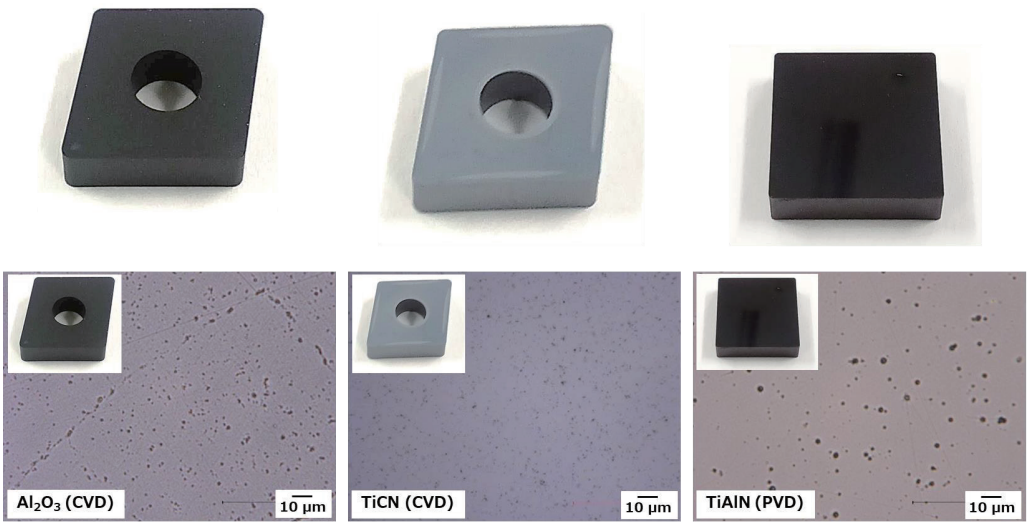

Fig. 1. (Color online) Surface observation photographs of Al_2O_3, TiCN, and TiAlN films.

were around 13 mm and 4.5 mm, respectively. The reason why the shapes of the substrates differed from each other is that the machines used for cutting were different. For the Al_2O_3 film sample, first, a TiCN film was deposited onto the WC-Co substrate by chemical vapor deposition (CVD). The TiCN film worked as an adhesive layer for depositing the Al_2O_3 film and its thickness was around 10 μm. Then, an Al_2O_3 film of 4 μm thickness was deposited using 0.35 vol.% H_2S and the remaining H_2. The substrate temperature and pressure during the CVD were set to be 1020 °C and 9.0 kPa, respectively, with mixed gases of 2.0 vol.% $AlCl_3$, 4.5 vol.% CO_2, and 2.2 vol.% HCl. The film deposition rate was 1.0 μm/h. For the TiCN film sample, a 5-μm-thick TiCN film was deposited onto the WC-Co substrate by CVD using mixed gases of 23 vol.% N_2, 1.3 vol.% $TiCl_4$, and 0.8 vol.% CH_3CN, and the remaining H_2. The substrate temperature and pressure were set to 820 °C and 7.5 kPa, respectively, and the film deposition rate was 0.9 μm/h. For the TiAlN film samples, the arc-ion plating technique, which is a type of physical vapor deposition (PVD), was employed to deposit the TiAlN film directly onto the WC-Co substrate. The deposition was conducted using a TiAl alloy target in N_2 gas at a pressure of 3–5 Pa. The bias voltage and arc current were set to be 50 V and 150 A, respectively. Under these conditions, the film deposition rate was maintained at 1.0 μm/h. The film thickness was around 3 μm. In the magnified photographs, many dark dots can be seen on the surfaces of all the films. Those are considered as some type of defect (e.g., droplets) formed during the deposition process.

Figure 2 shows a cross-sectional view of the Al_2O_3 sample as a process chart for a microcantilever beam. A commercial FIB system (SII Nano Technology, SMI3050) was used. First, the Al_2O_3 film surface was polished mechanically because the as-deposited film surface was slightly rough for fabricating a microcantilever beam using FIB. Second, the cantilever beam was processed using FIB. Third, the in-plane cantilever beam shape was roughly fabricated at the acceleration voltage of 30 kV. The beam current and diameter were set to be 13 nA and 2000 nm, respectively. Then, the vacancy beneath the cantilever beam was made under the same conditions as the last process, so that the thickness of the cantilever beam was 2.5 μm from the top surface of the evaluating film. After that, the sidewall and bottom surfaces were finely formed and made as smooth as possible using FIB under the conditions of 30 kV, 700 pA, and 60 nm for acceleration voltage, beam current, and beam diameter, respectively. In the case of the samples for the fracture toughness test, a precrack was introduced on the cantilever beam surface under the same above-mentioned conditions. In the scanning electron microscopy (SEM) images shown in Fig. 3(a), it was found that all the cantilever beams were finely formed using FIB as bending test samples. The width, length, and thickness were 10, 20, and 2.5 μm, respectively, which were precisely controlled using FIB. In the fracture toughness test samples shown in Fig. 3(b), it was found that a precrack was finely made using FIB in the vicinity of the fixed end of each cantilever beam. The precrack of 2 μm was processed from the fixed end. The depth varied from 0.15 to 1.0 μm to investigate the fracture toughness values place by place in the thickness direction. Concave portions, which were defects, were found on the top surface of each film. All the cantilever beam structures were processed to avoid those defects as much as possible because they were considered to be stress concentration spots during bending.

For strength and fracture toughness tests under bending, a commercial nanoindentation

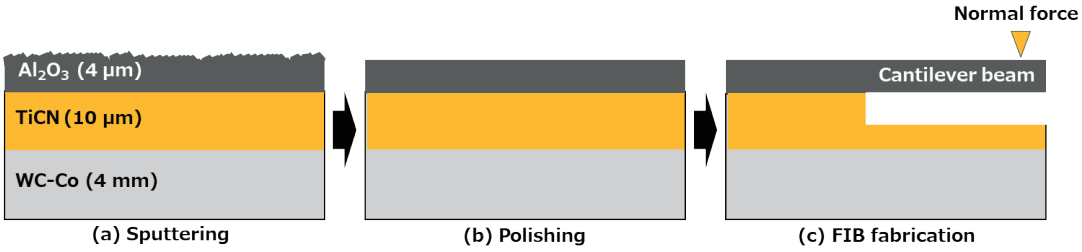

Fig. 2. (Color online) Schematic of process flow for fabricating a microcantilever sample for bending test.

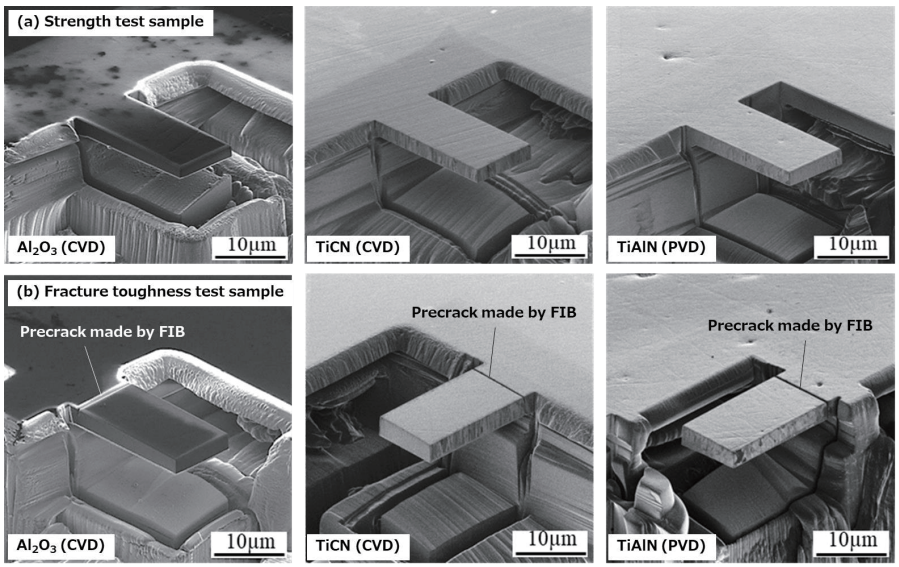

Fig. 3. SEM images of processed microcantilever samples for bending and fracture toughness tests.

system (Elionix, ENT-1100a) with a Berkovich indenter tip was used. The indenter tip was penetrated at 15 μm from the fixed end of each cantilever beam. Bending loading was performed at a constant loading rate of 10 nm/s. In the cantilever bending test, the relationship between bending force (F) and deflection (δ) is given by

$$F = (wt^3E)\delta/4l^3, \tag{1}$$

where w, t, and l are the width, thickness, and length of the cantilever beam, respectively, and E is Young's modulus. Here, l indicates the distance between the fixed end and the loading point (= 15 μm). The maximum tensile stress (σ_{max}) is generated on the top surface of the fixed end, which can be expressed as

$$\sigma_{max} = M/Z = 6Fl/wt^2, \tag{2}$$

where M and Z are the bending moment and section modulus, respectively. The fracture toughness (K_{IC}) in the cantilever beam with a notch can be expressed as an empirical equation:

$$K_{IC} = F_{max} l\alpha / wt^{3/2}, \tag{3}$$

$$\alpha = 1.46 + 24.36d/t - 47.21(d/t)^2 + 75.18(d/t)^3.^{(21)} \tag{4}$$

All the tests were conducted at 25 °C in ambient air.

3. Results and Discussion

Figure 4 shows a representative load–displacement relationship of microcantilever beams made of Al_2O_3, TiCN, and TiAlN films evaluated by the bending test. The displacement is indicative of the deflection at the loading point. It was found that the three microcantilever beams show a linear load–displacement relationship, indicating that all the materials fractured in a brittle manner during elastic deformation. In the case that the cantilever beam is thin and long, an indenter tip is known to slide before fracture owing to a large deflection. It provides a nonlinear load–displacement relationship. In this study, only linear relationships were obtained, which is evidence that the bending tests were correctly carried out. The microcantilever beams made of TiCN and TiAlN fractured at around 2 mN, whereas that made of Al_2O_3 fractured at over 5 mN, twice those of the other two materials. Five cantilever beams for each film were subjected to the bending test to evaluate their mechanical properties. The Young's moduli obtained in this study were 342 ± 51, 377 ± 42, and 367 ± 57 GPa for the Al_2O_3, TiCN, and

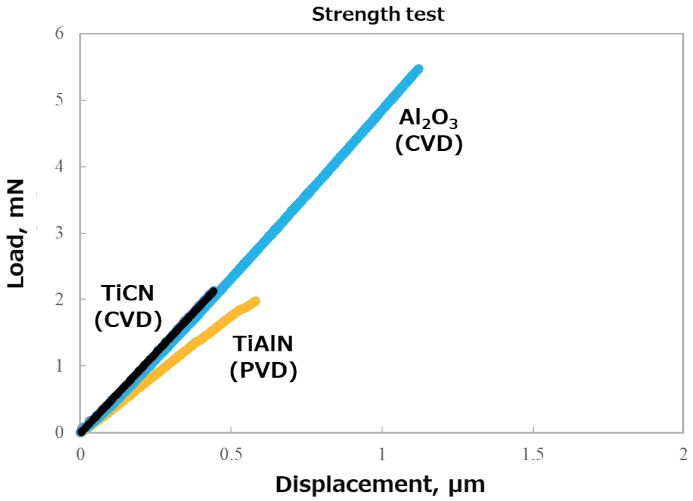

Fig. 4. (Color online) Representative load–displacement relationship obtained in microcantilever bending test.

TiAlN microcantilevers, respectively, which are almost comparable to their bulk values. The fracture strength of Al_2O_3 was 5.4 ± 0.8 GPa on average, which was almost twice those of TiCN and TiAlN (2.6 ± 0.5 and 2.9 ± 0.3 GPa, respectively). The reason why only Al_2O_3 showed high strength is that Al_2O_3 has higher purity and fewer defects than the others. TiCN is known as a high-purity hard coating film as well, but some defects are possibly included in the film. The TiAlN film, which is the sole PVD film in this study, is considered to possess droplets of around a few μm diameter, which would have affected the stress concentration site during bending.

Figure 5 shows representative fracture surfaces observed by SEM. The Al_2O_3 sample showed an irregular fracture surface. It was found that a river-like pattern from the top surface to the bottom can be seen, indicating that a crack initiated on the top surface and propagated to the bottom, which is typically observed in a brittle fracture. No intrinsic defects such as voids or surface notches were detected. The fracture surfaces of the other two samples showed a different trend from that of the Al_2O_3 sample. The fracture surface of the TiCN sample was found to consist of columnar structures. The diameter of each column was roughly estimated to be 100 nm, which was consistent throughout the film. Although the fracture origin and propagation direction were unclear because of its strong columnar structure, it was found that the cantilever beam showed brittle fracture. The TiAlN cantilever beam showed a columnar fracture surface similar to that of the TiCN beam, but the shape of each column was not as sharp as that of the TiCN film. This implies that the TiAlN film was denser than the TiCN film. Typically, the interface between columns is known to work as a stress concentration site, so thin films with clearer columns possess lower fracture strength. From the fracture surface comparison, it was found that the Al_2O_3 film was the densest among the three films, which would have provided high fracture strength that is almost twice those of the TiCN and TiAlN films.

Figure 6 shows a representative load–displacement relationship of microcantilever beams with a precrack. In those cases, the ratios of precrack depth to cantilever thickness were 0.4, 0.44, and 0.4 for the Al_2O_3, TiCN, and TiAlN cantilever beams, respectively. All the load–displacement relationships were found to be linear until fracture. All the samples fractured at the precrack portion. The slopes of the TiCN and TiAlN samples looked almost the same, whereas that of the Al_2O_3 sample was found to be smaller than those of the other two samples. This might be caused by the slightly smaller thickness of the Al_2O_3 sample than of the other two, leading to

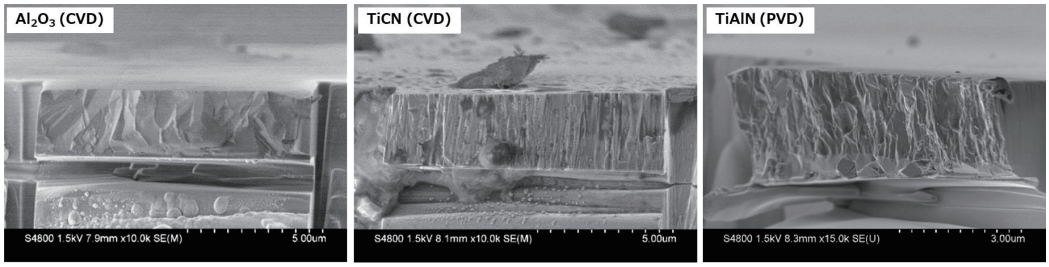

Fig. 5. SEM images of fracture surface after microcantilever bending test.

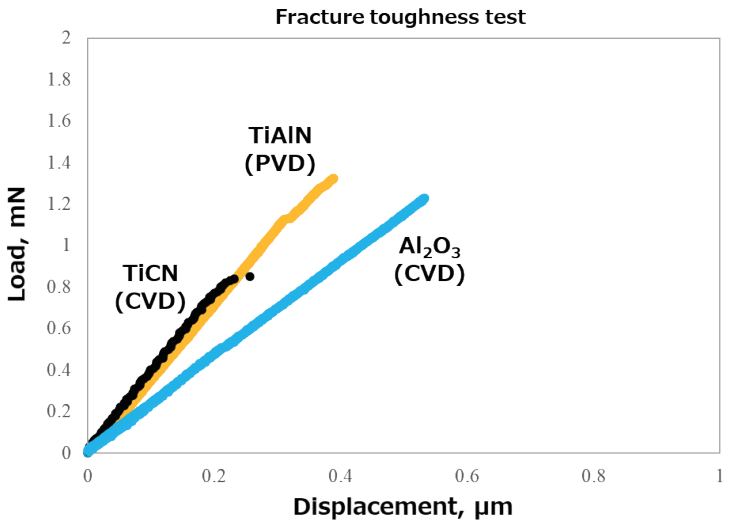

Fig. 6. (Color online) Representative load–displacement relationship obtained in fracture toughness test.

its higher flexibility. The TiAlN sample was found to show better mechanical resistance than the TiCN sample under the same precrack depth-to-thickness ratio. This indicates that the TiAlN film was mechanically tougher than the TiCN film.

Figure 7 shows fracture toughness as a function of the precrack depth-to-thickness ratio (d/t) of microcantilever beam samples. In the Al_2O_3 sample, the fracture toughness was measured to be 4.1 MPa√m at the d/t of 0.4. With a decreasing d/t, the fracture toughness was found to increase exponentially. At the d/t of 0.14, the fracture toughness took the maximum value of 5.5 MPa√m, which is 2.5–3.3 times higher than the literature value.[22] The difference between the maximum and minimum fracture toughness values was 2.2 MPa√m, indicating that the fracture toughness value differed from place to place in the thickness direction. The TiCN sample, deposited by CVD as well, was found to show a trend similar to the Al_2O_3 sample, although the magnitude of the fracture toughness was low by around 2.5 MPa√m at each d/t. On the other hand, the TiAlN sample, deposited by PVD, showed a different trend where the fracture toughness value stayed constant at around 3.0 MPa√m throughout the d/t range tested here. That is, it can be said that the PVD film showed no thickness dependence on fracture toughness.

On the basis of the experimental results, the following two things should be discussed. The first is about the reason why the Al_2O_3 film showed a higher fracture toughness than the TiAlN film. Considering the difference in thermal expansion coefficient between the Al_2O_3 film and the WC-Co substrate, tensile residual stress is probably included in the CVD film,[1] which is typically seen in hard coating films formed by CVD. In the case of TiCN, another CVD film evaluated in this study, Fig. 8 clearly shows that multiple cracks were introduced in the TiCN film in the bending fracture, although single cracking happened in the TiAlN film formed by PVD. This is evidence that the CVD film having tensile residual stress was weak against externally applied tensile stress, and brittle fracture happened easily. Actually, the TiCN film showed lower fracture toughness than the TiAlN film, which is considered to possess

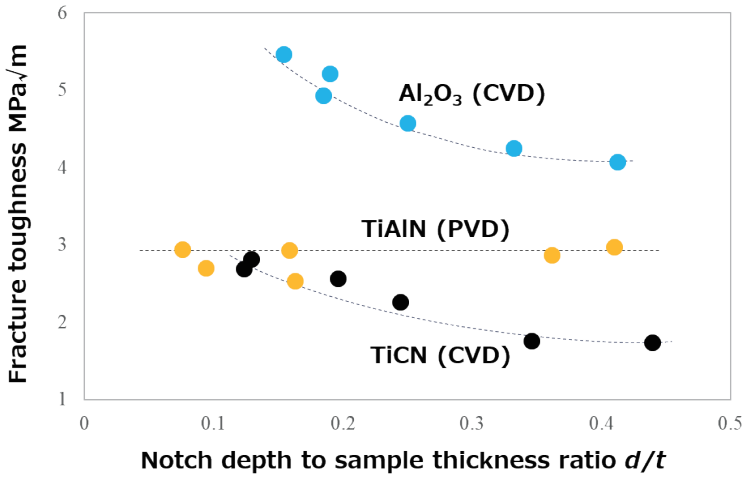

Fig. 7. (Color online) Fracture toughness as a function of notch depth-to-sample thickness ratio.

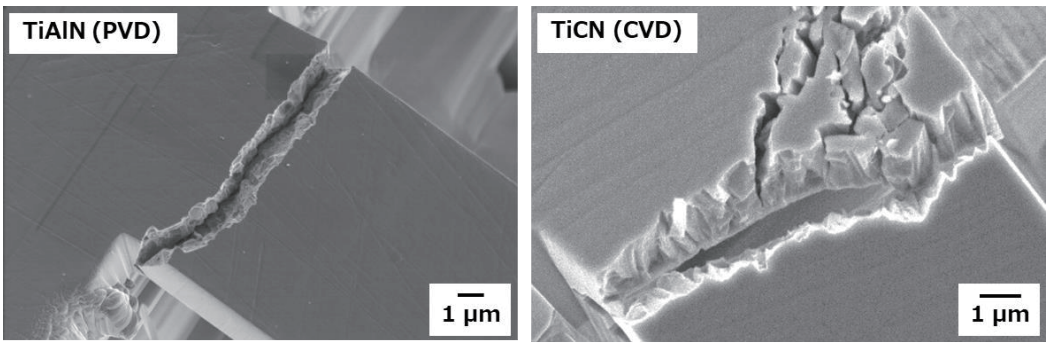

Fig. 8. SEM images of cracking introduced after microcantilever bending test.

compressive residual stress after PVD. Note, however, that the Al_2O_3 film showed higher fracture toughness than the other two films, although it had tensile residual stress. It might be attributed to grain size. As shown in Fig. 9, cross-sectional electron backscatter diffraction (EBSD) analyses suggest that the crystal grains in the Al_2O_3 film were definitely larger than those in the others. That is, the in-plane diameter ranged from 1 to 2 μm, roughly twice those of the others. In addition, the TiCN and TiAlN films possessed a columnar structure, whereas the Al_2O_3 film possessed a grained and noncolumnar structure. This structural difference might have provided high fracture toughness in the Al_2O_3 film. Moreover, the crystal orientation might have influenced the fracture toughness, although it was not precisely controlled during the deposition in this study.

The second one is about the thickness effect on fracture toughness seen in the two CVD films. Although the thickness effect was not obtained in the PVD film, it was clearly seen in the two CVD films. The thickness effect happened possibly because of the crystal grain size. In the EBSD results shown in Fig. 9, it was found that the grain size in the CVD films was different

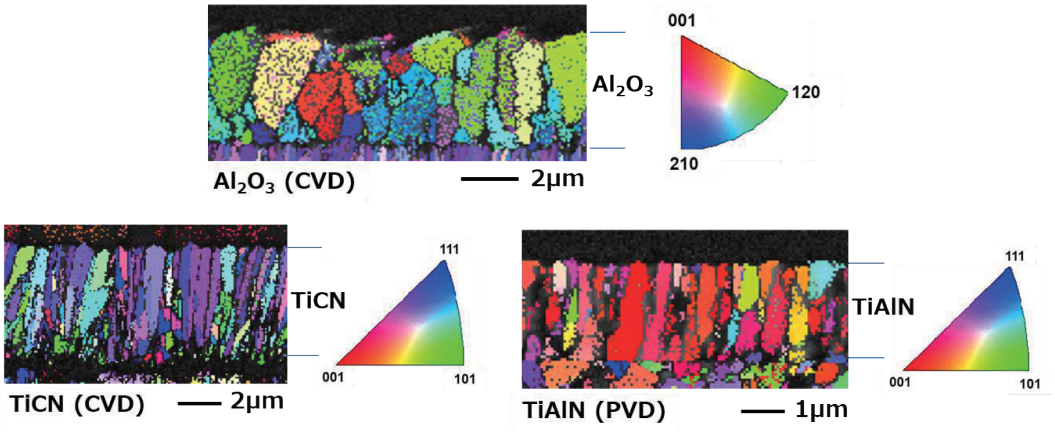

Fig. 9. (Color online) Cross-sectional EBSD image of Al2O3, TiCN, and TiAlN films.

from place to place in the thickness direction. Although the crystal grain in the vicinity of the substrate was smaller than 1 μm at least, it grew during the deposition process until it finally became 1 or 2 μm on the top surface. On the other hand, in the PVD film, the diameter of each crystal column looks almost constant throughout its thickness direction. In the CVD process, a film is deposited in an epitaxial-like manner more than in the PVD process.[23] In epitaxial growth, since the crystallinity of the deposited film follows that of a substrate, the crystal grain size increases as the deposition proceeds. It means that the crystal grain in the vicinity of the top surface of a film is definitely larger than that at the bottom.[1] This "grain size nonuniformity" might have provided the "fracture toughness nonuniformity" in the out-of-plane direction. However, this should not be concluded until the relationship between grain size and fracture toughness has been experimentally found and analyzed.

4. Conclusions

In this study, the mechanical properties of hard coating films were evaluated by a microcantilever bending test. CVD was employed for forming Al_2O_3 and TiCN films, and PVD was employed for forming a TiAlN film. The Young's modulus ranged from 340 to 379 GPa, with no significant difference among the films, whereas the fracture strength of the Al_2O_3 film was 5.5 GPa, almost twice those of the other two films. In the fracture toughness test, the two CVD films showed thickness dependence on fracture toughness, whereas the PVD film showed a constant value irrespective of precrack depth. The Al_2O_3 film having tensile residual stress possessed a maximum fracture toughness of 5.5 MPa$\sqrt{m}$, which was higher than that of the TiAlN film having compressive residual stress. The reason was discussed considering the crystal grain size and orientation.

Mechanical characterization of hard coating films is known to be difficult technically. In this study, the microcantilevers made of Al_2O_3, TiCN, and TiAlN films were fabricated using FIB,

and the bending test was conducted using a nanoindentation tester. The combination of the FIB process and nanoindentation demonstrated that the mechanical characterization of hard coating films could be carried out well, and we were able to discuss the differences in strength and fracture toughness among the three films.

References

1 S. Ruppi: Surf. Coat. Technol. **202** (2008) 4257. https://doi.org/10.1016/j.surfcoat.2008.03.021
2 H. Chien, C. Diaz-Jimenez, G. S. Rohrer, Z. Ban, P. Prichard, and Y. Liu: Surf. Coat. Technol. **215** (2013) 119. https://doi.org/10.1016/j.surfcoat.2012.07.088
3 S. Rodriguez-Barrero, J. Fernandez-Larrinoa, I. Azkona, L. N. Lopez de Lacalle, and P. Polvorosa: Mater. Manuf. Processes **31** (2016) 593. https://doi.org/10.1080/10426914.2014.973582
4 A. van der Rest, H. Idrissi, F. Henry, A. Favache, D. Schryvers, J. Proost, J-P. Raskin, Q. V. Overmeere, and T. Pardoen: Acta Mater. **125** (2017) 27. http://dx.doi.org/10.1016/j.actamat.2016.11.037
5 C. Cibert, H. Hidalgo, C. Champeaux, P. Tristant, C. Tixier, J. Desmaison, and A. Catherinot: Thin Solid Films **516** (2008) 11290. https://doi.org/10.1016/j.tsf.2007.05.064
6 T. Tsuchiya, O. Tabata, J. Sakata, and Y. Taga: J. Microelectromech. Syst. **7** (1998) 106. https://doi.org/10.1109/84.661392
7 K. Sato, M. Shikida, M. Yamasaki, and T. Yoshioka: Proc. IEEE MEMS 1996 (San Diego, 1996) 360–364. https://doi.org/10.1109/MEMSYS.1996.494008
8 T. Yi and C. J. Kim: Meas. Sci. Technol. **10** (1999) 706. https://doi.org/10.1088/0957-0233/10/8/305
9 Y. Isono, T. Namazu, and N. Terayama: J. Microelectromech. Syst. **15** (2006) 169. https://doi.org/10.1109/JMEMS.2005.859196
10 T. Namazu, S. Inoue, H. Takemoto, and K. Koterazawa: IEEJ Trans. on Sen. Micromach. **125** (2005) 374. https://doi.org/10.1541/ieejsmas.125.374
11 T. Namazu and S. Inoue: Fatigue Fract. Eng. Mater. Struct. **30** (2007) 13. https://doi.org/10.1111/j.1460-2695.2006.01043.x
12 T. Namazu and Y. Isono: J. Microelectromech. Syst. **18** (2009) 129. https://doi.org/10.1109/JMEMS.2008.2008583
13 M. Fujii, T. Namazu, H. Fujii, K. Masunishi, Y. Tomizawa, and S. Inoue: J. Vac. Sci. Technol. B **30** (2012) 031804. https://doi.org/10.1116/1.4711040
14 T. Namazu, M. Fujii, H. Fujii, K. Masunishi, Y. Tomizawa, and S. Inoue: J. Microelectromech. Syst. **22** (2013) 1414. https://doi.org/10.1109/JMEMS.2013.2257985
15 T. Namazu: IEEJ Trans. Electr. Electron. Eng. **18** (2023) 308. https://doi.org/10.1002/tee.23747
16 T. Fujii, T. Namazu, K. Sudoh, S. Sakakihara, and S. Inoue: J. Eng. Mater. Technol. **135** (2013) 051002. https://doi.org/10.1115/1.4024545
17 H-P. Phan, T. Kozeki, T. Dinh, T. Fujii, A. Qamar, Y. Zhu, T. Namazu, N-T. Nguyen, and D. V. Dao: RSC Adv. **5** (2015) 82121. https://doi.org/10.1039/C5RA13425K
18 T. Kozeki, H-P. Phan, D. V. Dao, S. Inoue, and T. Namazu: Jpn. J. Appl. Phys. **55** (2016) 06GL02. https://doi.org/10.7567/JJAP.55.06GL02
19 G. Ina, T. Fujii, T. Kozeki, E. Miura, S. Inoue, and T. Namazu: Jpn. J. Appl. Phys. **56** (2017) 06GN17. https://doi.org/10.7567/JJAP.56.06GN17
20 H. Ando and T. Namazu: J. Vac. Sci. Technol. B **41** (2023) 062808. https://doi.org/10.1116/6.0002983
21 M. Bartosik, C. Rumeau, R. Hahn, Z. L. Zhang, and P. H. Mayrhofer: Sci. Rep. **7** (2017) 16476. https://doi.org/10.1038/s41598-017-16751-1
22 D. W. Stollberg, J. M. Hampikian, L. Riester, and W. B. Carter: Mater. Sci. Eng., A **359** (2003) 112. https://doi.org/10.1016/S0921-5093(03)00339-3
23 A. Ito: J. Ceram. Soc. Jpn. **129** (2021) 646. http://doi.org/10.2109/jcersj2.21135

About the Authors

Takahiro Namazu received his B.S., M.S., and Ph.D. degrees in mechanical engineering from Ritsumeikan University, Kusatsu, Japan, in 1997, 1999, and 2002, respectively. From 2002 to 2006, he was an assistant professor at the Department of Mechanical and Systems Engineering, Graduate School of Engineering, University of Hyogo, Himeji, Japan. In 2007, he became an associate professor at the university. In 2010, he joined the Precursory Research for Embryonic Science and Technology (PRESTO) program, "Nanosystems and Emergent Functions" of the Japan Science and Technology Agency (JST), as a researcher. In 2016, he became a professor at the Department of Mechanical Engineering, Aichi Institute of Technology, Toyota, Aichi, Japan. In 2020, he became a professor at the Faculty of Engineering, Kyoto University of Advanced Science (KUAS). He is currently engaged in studies on functional film materials, such as self-propagating exothermic materials, and their applications to micro/nano-electro-mechanical systems (NMEMS). His research interests also include the development of material testing techniques for measuring the mechanical properties of micro/nanoscale materials, such as carbon nanotubes and silicon nanowires, with a focus on clarifying the nanomaterials' size effect phenomena. The evaluation of the reliability of MEMS and semiconductor devices is among his interests towards realizing the design of ultralong-life microdevices. (namazu.takahiro@kuas.ac.jp)

Tomohide Ide received his B.E. and M.E. degrees from Aichi Institute of Technology, Japan, in 2018 and 2020, respectively. His research interests are the development of mechanical characterization techniques for hard-coating thin-film materials and the measurement of the mechanical properties of materials used for MEMS and semiconductor devices. He is also interested in developing functional materials, such as shape memory alloy films and self-propagating exothermic films, by sputtering.

Tsuyoshi Yamasaki received his B.E. degree from Gifu University in 2009. In 2009, he joined Kyocera Corporation. From 2009 to 2021, he was mainly engaged in the development of hard thin films at the Cutting Tool Materials R&D Division of Kyocera Corporation. Since 2021, he has been working on the crystal growth of nitride semiconductors in the R&D Division. His research field is power devices.

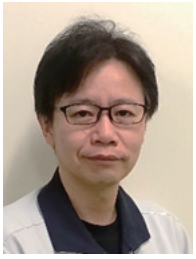

Takahito Tanibuchi received his B.S. and M.S. degrees from Ritsumeikan University in 1999 and 2001, respectively. He joined Kyocera Corporation in 2001. He has been engaged in the development of materials for metal cutting tools at the Cutting Tool Materials R&D Division of Kyocera Corporation since 2001. His research interests are in hard coatings and ceramics with excellent mechanical properties and heat resistance.